AUTHOR QUERY FORM

ELSEVIER	**Journal:** SYNMET **Article Number:** 14849	**Please e-mail or fax your responses and any corrections to:** **E-mail:** corrections.esch@elsevier.thomsondigital.com **Fax:** +353 6170 9272

Dear Author,

Please check your proof carefully and mark all corrections at the appropriate place in the proof (e.g., by using on-screen annotation in the PDF file) or compile them in a separate list. Note: if you opt to annotate the file with software other than Adobe Reader then please also highlight the appropriate place in the PDF file. To ensure fast publication of your paper please return your corrections within 48 hours.

For correction or revision of any artwork, please consult http://www.elsevier.com/artworkinstructions.

Any queries or remarks that have arisen during the processing of your manuscript are listed below and highlighted by flags in the proof. Click on the 'Q' link to go to the location in the proof.

Location in article	Query / Remark: click on the Q link to go Please insert your reply or correction at the corresponding line in the proof
Q1	Please confirm that given names and surnames have been identified correctly.
Q2	"Your article is registered as a regular item and is being processed for inclusion in a regular issue of the journal. If this is NOT correct and your article belongs to a Special Issue/Collection please contact k.selvaraj@elsevier.com immediately prior to returning your corrections."
Q3	Please check the edits made in the sentence "The samples were..." and amend if necessary.
Q4	Please check the edits made in the Eq. (1), and amend if necessary.
Q5	One or more sponsor names and the sponsor country identifier may have been edited to a standard format that enables better searching and identification of your article. Please check and correct if necessary.
	Please check this box or indicate your approval if you have no corrections to make to the PDF file ☐

Thank you for your assistance.

Synthetic Metals xxx (2015) xxx–xxx

Contents lists available at ScienceDirect

Synthetic Metals

journal homepage: www.elsevier.com/locate/synmet

1 Graphical abstract

Synthetic Metals xxx (2015) xxx–xxx

Characterization and electrochemical properties of conducting nanocomposites synthesized from *p*-anisidine and aniline with titanium carbide by chemical oxidative method

I. Radja[a], H. Djelad[a,b], E. Morallon[b], A. Benyoucef[a,*]

[a] *Laboratoire de Chimie Organique, Macromoléculaire et des Matériaux, Université de Mascara. Bp 763, Mascara 29000, Algeria*
[b] *Departamento de Química Física e Instituto Universitario de Materiales, Universidad de Alicante, Apartado 99, E-03080 Alicante, Spain*

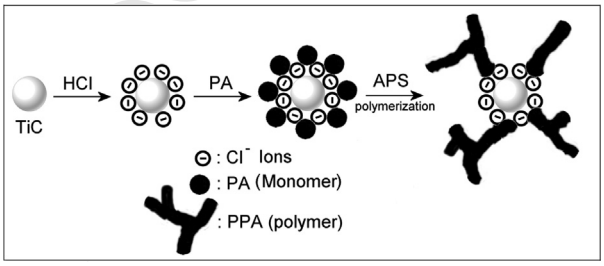

G Model
SYNMET 14849 1
ARTICLE IN PRESS

Synthetic Metals xxx (2015) xxx–xxx

Contents lists available at ScienceDirect

Synthetic Metals

journal homepage: www.elsevier.com/locate/synmet

1 Highlights

Synthetic Metals xxx (2015) xxx–xxx

Characterization and electrochemical properties of conducting nanocomposites synthesized from *p*-anisidine and aniline with titanium carbide by chemical oxidative method

I. Radja [a], H. Djelad [a,b], E. Morallon [b], A. Benyoucef [a,*]

[a] *Laboratoire de Chimie Organique, Macromoléculaire et des Matériaux, Université de Mascara. Bp 763, Mascara 29000, Algeria*
[b] *Departamento de Química Física e Instituto Universitario de Materiales, Universidad de Alicante, Apartado 99, E-03080 Alicante, Spain*

- A simple and facile method was used to synthesize prepared a nanocomposite.
- Intercalation of monomers on TiC was followed by oxidative polymerization.
- Characterizations confirm the presence of polymers on TiC.
- The PPA/TiC are more thermally stable than those of PANI/TiC.
- Good electrochemical response has been observed for polymers grown on TiC.

G Model
SYNMET 14849 1–8
ARTICLE IN PRESS

Synthetic Metals xxx (2015) xxx–xxx

Contents lists available at ScienceDirect

Synthetic Metals

journal homepage: www.elsevier.com/locate/synmet

Characterization and electrochemical properties of conducting nanocomposites synthesized from *p*-anisidine and aniline with titanium carbide by chemical oxidative method

Q1 I. Radja[a], H. Djelad[a,b], E. Morallon[b], A. Benyoucef[a,*]

[a] Laboratoire de Chimie Organique, Macromoléculaire et des Matériaux, Université de Mascara. Bp 763, Mascara 29000, Algeria
[b] Departamento de Química Física e Instituto Universitario de Materiales, Universidad de Alicante, Apartado 99, E-03080 Alicante, Spain

ARTICLE INFO

Article history:
Received 10 July 2014
Received in revised form 2 January 2015
Accepted 26 January 2015
Available online xxx

Keywords:
Nanocomposite
Nanoparticle
Conducting polymer
Titanium carbide
Electrochemical studies

ABSTRACT

A novel polymer/TiC nanocomposites "PPA/TiC, poly(PA-*co*-ANI)/TiC and PANI/TiC" was successfully synthesized by chemical oxidation polymerization at room temperature using *p*-anisidine and/or aniline monomers and titanium carbide (TiC) in the presence of hydrochloric acid as a dopant with ammonium persulfate as oxidant. These nanocomposites obtained were characterized by Fourier transform infrared (FTIR) spectroscopy, X-ray diffraction (XRD), transmission electron microscopy (TEM), energy dispersive spectroscopy (EDS), and thermogravimetric analysis (TGA). XRD indicated the presence of interactions between polymers and TiC nanoparticle and the TGA revealed that the TiC nanoparticles improve the thermal stability of the polymers. The electrical conductivity of nanocomposites is in the range of 0.079–0.91 S cm^{-1}. The electrochemical behavior of the polymers extracted from the nanocomposites has been analyzed by cyclic voltammetry. Good electrochemical response has been observed for polymer films; the observed redox processes indicate that the polymerisation on TiC nanoparticles produces electroactive polymers. These nanocomposite microspheres can potentially used in commercial applications as fillers for antistatic and anticorrosion coatings.

1. Introduction

Intrinsically conducting polymer thin films have been used in various kinds of electronic devices. Conducting polymers are combined with metal oxides because of their enhanced physical and electronic properties and find useful applications in different devices, such as sensors, electrodes, batteries, and photovoltaics [1,2]. Conducting-polymer-based solar cells have gained much importance in the last decade because of their low cost, easy processability, low toxicity, and high environmental stability [3,4]. Among conducting polymers, polyaniline (PANI) is unique because it can be easily doped with various acids and it also exhibits good thermal and environmental stabilities [5,6]. Metal oxides can also replace fullerenes (electron-acceptor materials) in bulk heterojunction solar cells because of their high electron mobilities [1,2].

Organic–inorganic hybrid materials, which combine excellent performances of the two materials, are extremely innovative, and such materials promise new applications in many fields, such as electronics, optics, electrochemistry, supercapacitor, mechanics and biology [7–10]. Any organic–inorganic hybrid materials can be obtained by intercalative reactions of layered solids based on self-assembly approaches [11–14].

Recently, on the basis of conducting polymers and inorganic nanoparticles, the nanocomposites have attracted attention as it seems to be the potential route to improve the performance of materials in devices. Several reports on the synthesis of the nanocomposites of polyaniline with Fe_3O_4 [15], ZnO [16], ZrO_2 [17], TiO_2 [18] and montmorillonite [19] nanoparticles have already been published.

Titanium carbide (TiC) is one of the most important metal carbides with excellent properties, such as high melting temperature, hardness, strength, wear, corrosion resistance, electrical conductivity, and thermal conductivity [20,21]. TiC is an important material from technological applications because of its high melting point, hardness, elastic modulus, electrical conductivity and low coefficient of thermal expansion. Composite systems consisting of a polymer matrix and conductive particles of titanium carbide have been considered as a novel class of smart materials, because of their ability to switch from negative to positive temperature coefficient of conductivity [22–25]. Negative temperature coefficient of conductivity (NTCC) is useful in applications such as self controlled heaters, current limiters,

* Corresponding author. Tel.: +213 771707184; fax: +213 45930118.
E-mail address: ghani29000@yahoo.fr (A. Benyoucef).

http://dx.doi.org/10.1016/j.synthmet.2015.01.028
0379-6779/© 2015 Published by Elsevier B.V.

sensors, thermistors and over current protectors, while it is considered as detrimental in cable engineering [26].

Moreover, the synthesis of poly(*p*-anisidine)/TiC (PPA/TiC), poly (*p*-anisidine-*co*-aniline)/TiC (poly(PA-*co*-ANI)/TiC) and PANI/TiC nanocomposites has not been reported before. Herein, we look forward to synthesis nanocomposites by using an in-situ chemical polymerization route and used it as new material and characterized by UV–vis, FT-IR, XRD, thermogravimetric analysis (TGA) and further study for electrochemical properties. The *p*-anisidine is a substituted derivative of PANI with methoxy ($-OCH_3$) group substituted at *para* positions. The PPA was chosen as an organic counterpart for this study to explore the possibility of utilizing it as an alternative to PANI for technologies application. The purpose of this paper is to give a preliminary account of our research on the use of polymer/TiC nanocomposites as suitable anodic materials Q2 for hydrometal lurgy.

2. Experimental

2.1. Materials

The monomers aniline (ANI) (from Aldrich) was distilled under vacuum prior to use and *p*-anisidine (PA) (from Aldrich) was used as received. Perchloric acid and hydrochloric acid (from Merck) was Suprapur quality and all the solutions were freshly prepared with distilled-deionised water was obtained from an Elga Labwater Purelab Ultra system. A titanium carbide (TiC) (99%) is purchased from the Sigma–Aldrich Company. Ammonium persulfate ($(NH_4)_2S_2O_8$) (APS) and ammonia solution (NH_4OH) were all of analytical purity and used without further purification.

2.2. Chemical synthesis of nanocomposites

In the preparation of PPA/TiC nanocomposite process, firstly, TiC nanoparticles (1.0 g) were dispersed in 1 M HCl aqueous solution with ultrasonic vibration for 1 h to obtain a uniform suspension. A 1.35 g quantity of PA monomer was added to this mixture dropwise under strong stirring in an ice-water bath and stirred for 1 h. Then 2.51 g of APS in 20 mL of 1 M HCl solution was slowly added dropwise to the suspension mixture (using 1:1 monomer/oxidant mole ratio), and the solution was stirred at room temperature for 24 h. A solid product was obtained after filtration and washed with 1 M HCl and deionized water to remove residual aniline and ammonium sulfate. The final products were bathed using 50 mL of 1 M NH_4OH at room temperature while magnetically stirring for 2 h. The product was collected by filtering and washing the precipitate with deionized water, and dried under vacuum at 60 °C for 24 h [27,28].

For the synthesis of the PANI/TiC and poly(PA-*co*-ANI)/TiC nanocomposites and also the polymer PPA (without TiC), the same procedure was repeated.

2.3. Nanocomposite characterization

The X-ray diffraction of the powder nanocomposites were taken using a Bruker CCD-Apex equipment with a X-ray generator (Cu Ka and Ni filter) operated at 40 kV and 40 mA. For recording the UV–vis absorption spectra, a Hitachi U-3000 spectrophotometer was used. The solution of the homo- and co-polymer in *N*-methyl-2-pyrrolidone (NMP) was used for recording the spectrum. Fourier transform infrared (FT-IR) spectroscopy was recorded using a Bruker Alpha in transmission mode after dissolving the sample in dried KBr.

Transmission electron microscopy (TEM) was performed to determine the morphology of the samples using JEOL microscope, JEM-2010 model. This TEM microscope is equipped with an X-ray detector Bruker XFlash 3001 for microanalysis energy dispersive spectroscopy (EDS) for the elucidation of chemical composition of the samples. A simultaneous TG-DTA (METTLER TOLEDO model TGA/SDTA851e/SF/1100) thermogravimetric analyzer was employed to perform the termal analysis under a 100 mL/min nitrogen flow at 10 °C/min until 900 °C.

2.4. Electrochemical studies

The electrochemical behaviour of the polymers was studied by cyclic voltammetry after their extraction from the polymer by dissolving in the *N*-methyl-2-pyrrolidone (NMP). It is known that this kind of conducting polymers is soluble in NMP [14,29], while the TiC remains in solid state. Thus, both components can be separated by filtration. The electrochemical measurements were carried out using a conventional cell of three electrodes. The counter and reference electrodes were a platinum foil and a hydrogen reversible electrode (RHE), respectively. For all the electrochemical and spectroelectrochemical experiments the polymers were separated from the catalyst by dissolving the mixture in NMP. Then polymer films were obtained by casting a drop of these solutions over the working graphite carbon electrode and heating with an infrared lamp to remove the solvent. The electrolyte used was 1 M $HClO_4$ and all experiments were carried out at 50 mV/s.

2.5. Electrical conductivity measurements

Electrical conductivity measurements were carried out using a Lucas Lab resistivity equipment with four probes in-line. The samples were dried in vacuum during 24 h and pellets of 0.013 m diameter were prepared using a FTIR mold by applying a pressure of 7.4, 10^8 Pa. Q3

3. Results and discussion

3.1. XRD characterization

Fig. 1 shows the X-ray diffractograms for all the three nanocomposites and TiC pure. The XRD pattern of the TiC particles presents the hexagonal structure with no extra reflections, and perfectly indexed to (0 0 1), (1 0 0), (1 0 n1), (1 1 0), (0 0 2), (1 1 1), (2 0 0), (1 0 2) and (2 0 1) crystal plane of hexagonal TiC (JCPDS Card No. 720097). In XRD of nanocomposites, all the peaks of TiC are observed. The XRD pattern for the polymer/TiC shows new low diffraction peaks at $2\theta = 22.81°$ (Fig. 1, insight). In addition, the intensities of this broad diffraction peak corresponding to polymer "PA, poly(PA-*co*-ANI) and PANI" in the nanocomposite become weakened with introducing TiC nanoparticles, which indicates that TiC nanoparticles have an effect on the crystallinity of polymer [30]. This indicates that the crystal structure of TiC is not modified due to the presence of polymer. This result also shows the interaction between the TiC nanoparticles and polymer molecular chains due to the adsorption of polymer molecular chains on the surface of the TiC nanoparticles.

The average crystallite sizes of TiC nanoparticles, and the three samples of nanocomposites were estimated from the X-ray diffraction patterns using Scherrer formula [31]: Q4

$$d = \frac{k \times \lambda}{\beta \times \cos\theta} \quad (1)$$

where d is the average crystallite size, λ is the X-ray wavelength, β is the full-width at half-maximum and θ is the diffraction angle. The value of k depends on several factors, including the Miller index of reflection plane and the shape of the crystal. If shape is

Please cite this article in press as: I. Radja, et al., Characterization and electrochemical properties of conducting nanocomposites synthesized from *p*-anisidine and aniline with titanium carbide by chemical oxidative method, Synthetic Met. (2015), http://dx.doi.org/10.1016/j.synthmet.2015.01.028

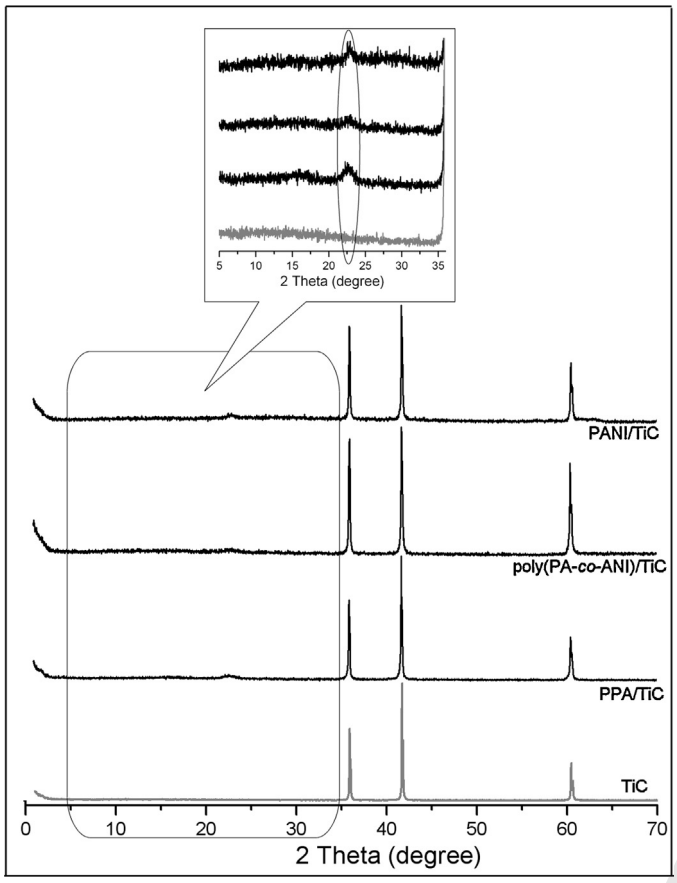

Fig. 1. XRD diffraction patterns of PPA/TiC, poly(PA-*co*-ANI)/TiC and PANI/TiC nanocomposites and TiC nanoparticles.

unknown, *k* is often assigned a value of 0.9. So the crystallite size of TiC nanoparticle, and the nanocomposites was computed from XRD patterns see Table 1.

3.2. FT-IR spectroscopy

The typical FT-IR spectra for TiC, pure PPA, pure PANI and PPA/TiC, poly(PA-*co*-ANI)/TiC, PANI/TiC nanocomposites containing 5 wt% TiC nanoparticles are shown in Fig. 2.

The characteristic bands for pure PPA are observed in the spectrum at 3425, 2935, 1207, 1169 and 800 cm^{-1}, in agreement with the reported literature [32]. The bands at approximately 1498 and 1591 cm^{-1} are due to the benzenoid and quinoid ring units, respectively. It was found that the PPA film formed by galvanostatic conditions contained both benzenoid and quinoid moieties. There are other characteristic bands at 1275 and 1114 cm^{-1}, due to 1,2,4-trisubstituted benzene rings. The characteristic bands of pure PANI were assigned as follows: at 3450 cm^{-1} it was associated to N—H stretching mode, C=N and C=C stretching modes for the quinoid and benzenoid rings are observed at 1573 cm^{-1} and 1480 cm^{-1} respectively, the bands at about 1309 cm^{-1} and 1243 cm^{-1} can been associated to C—N stretching mode for the benzenoid ring, while the band at 1126 cm^{-1} was assigned to a in plane bending vibration of C—H (mode of N=Q=N, Q=N^{+}H—B and B—N^{+}H—B), which was formed during protonation [33].

Table 1
The average crystallite size of the TiC nanoparticle and the three nanocomposites was computed from Scherrer formula.

Samples	TiC	PPA/TiC	poly(PA-*co*-ANI)/TiC	PANI/TiC
d (nm)	30.80	46.64	31.73	42.45

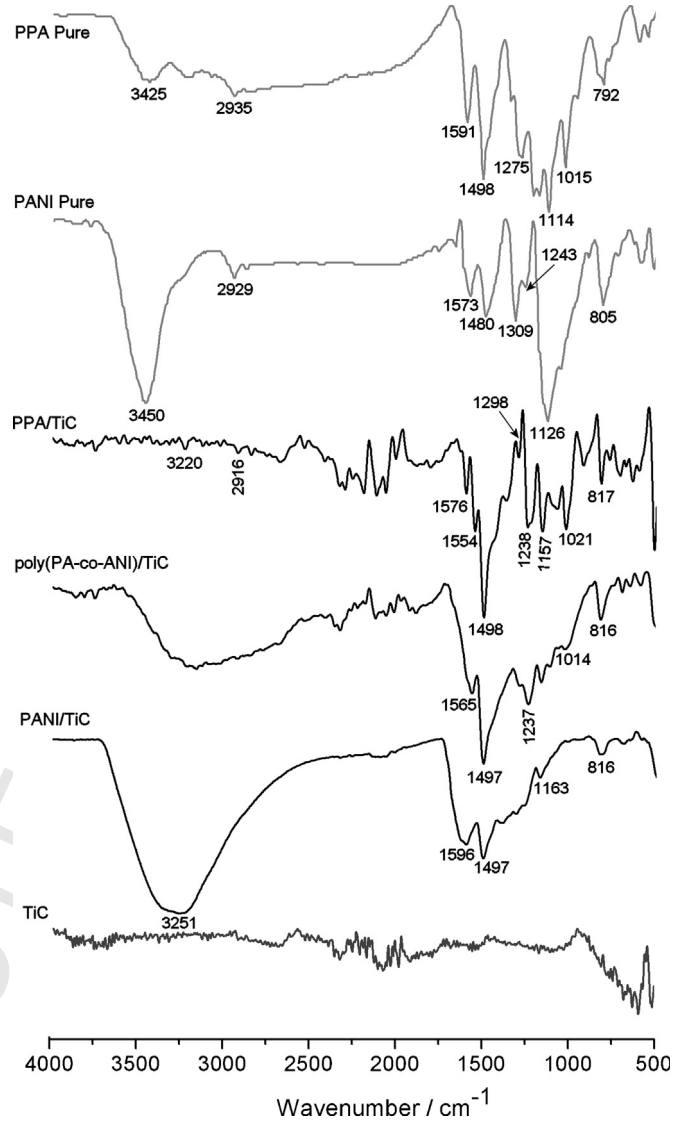

Fig. 2. FT-IR spectra of nanocomposites (PPA/TiC, poly(PA-*co*-ANI)/TiC and PANI/TiC), pure polymers (PPA and PANI) and TiC nanoparticles.

It was evident that the FTIR spectra of the nanocomposites (PPA/TiC, poly(PA-*co*-ANI)/TiC, PANI/TiC) contained contributions from both TiC and polymers. However, some bands of doped polymer had shifted due to interactions with TiC nanoparticles. For example, in PPA/TiC nanocomposite, the bands at 1275 cm^{-1}, 1215 cm^{-1} and 1169 cm^{-1} corresponding to the stretching mode of C—C, C—N and C—H, all shifted to higher wavenumbers, and C=N stretching band at 1591 cm^{-1} shifted to lower wavenumber. Similarly, the band at 3425 cm^{-1} also shifted to 3220 cm^{-1} this band was attributable to N—H stretching mode. These changes suggest that C—C, C—N and C—H bands became stronger in PPA/TiC nanocomposite, but the N—H band became weaker. This was probably because of the action of hydrogen bonding between the surfaces of TiC nanoparticles and the N—H groups in PPA polymer. And the presence of TiC nanoparticles had effect on the doping of PPA.

The spectra of poly(PA-*co*-ANI)/TiC and PANI/TiC nanocomposites, display bands between 1565–1596 cm^{-1} and 1497 cm^{-1} (ν(C=N) and ν(C=C)), indicating that the PA-*co*-ANI and ANI

Please cite this article in press as: I. Radja, et al., Characterization and electrochemical properties of conducting nanocomposites synthesized from *p*-anisidine and aniline with titanium carbide by chemical oxidative method, Synthetic Met. (2015), http://dx.doi.org/10.1016/j.synthmet.2015.01.028

Table 2
The electrical conductivity values of PPA/TiC, poly(PA-*co*-ANI)/TiC and PANI/TiC nanocomposites and polymers pure.

Samples	PPA/TiC	Poly(PA-*co*-ANI)/TiC	PANI/TiC	PPA	poly(PA-*co*-ANI)	PANI
Conductivity ($S\,cm^{-1}$)	0.08	0.09	0.91	0.22	0.82	1.45

polymers are present in the matrix. The spectra also display a broad band between 3251 cm^{-1}.

The increases in the intensity of the band between 1014 cm^{-1} and 1021 cm^{-1} corresponding to the stretching mode of C—O—C may be attributed to the represent the signal from the methoxy group in the anisidine [34].

Despite the slight shifts of these bands compared with the matrix, we can suppose that the overall framework is preserved after the reaction, in agreement with the X-ray powder diffraction data (Fig. 1).

3.3. Electrical conductivity characterization

Table 2 shows the electrical conductivities of nanocomposites that are in the range of 0.12–1.45 $S\,cm^{-1}$. An increase in the content of aniline in the polymerization produces the increase in conductivity. In the case of nanocomposites a reduction in the electrical conductivity is observed as compared to the pure polymers. This fact can be explained by the interactions between the polymers and TiC nanoparticles which probably led to the reduction in conjugation length of polymers [35–37]. Moreover, the presence of TiC nanoparticles hindered the transport of carriers between different molecular chains of polymer [37,38]. The presence of TiC particles may also have hindered the transfer of carriers between molecular chains of polymers.

3.4. UV–vis spectroscopy

Fig. 3 shows the UV–vis absorption spectra of PPA/TiC, poly(PA-*co*-ANI)/TiC and PANI/TiC nanocomposites, this samples dissolved in NMP solution for separate the polymer from TiC. Although the three samples show two characteristic absorption bands, the three spectra look somewhat different. The absorption bands at ~317–329 nm can be ascribed to π–π* transition of the benzenoid rings, whereas the bands at ~443–545 nm can be attributed to polaron–π* transition [39]. Therefore, it can be concluded from the UV–vis absorption spectrum of PPA/TiC that the doped state can be enhanced with the incorporation of PA units in the polymer chain, which may resulted with a strong electronic effect that can stabilize the doping state of polymer. Based on the previous research, the doping level can roughly be estimated from the absorption spectra of PPA/TiC at 450 nm (π–π* transition). The poly(PA-*co*-ANI)/TiC exhibits this band at higher wavelength which implies that the doping level of copolymer nanocomposite is lower than that of homopolymer nanocomposites.

This is in consistent with the results of FTIR spectra. When comparing the absorption spectra, a notable red shift of the bands are observed for copolymer poly((PA-*co*-ANI)/TiC nanocomposite as compared to homopolymers nanocompositess. This indicates a higher conjugation length appearing in copolymer nanocomposite. The effective conjugation length favors planar chain structures and steric factors that prevent to give twisted chains. Evidently, the steric hindrance connected with $-OCH_3$ substituent results in twisting, thus lowering the conjugation length in PPA [40]. These results suggest that the proportion of PA perhaps plays a significant role toward the determination of the chain length and other properties of these conducting copolymers.

3.5. Thermogravimetric analysis (TGA)

The thermal stability of a conducting polymer is very important for its potential application. Thermogravimetry (TGA) is a significant and useful dynamic way to detect the degradation behavior in which the weight loss of a polymer sample is measured continuously while the temperature is changed at a constant rate. In order to investigate the thermal stability of the PPA/TiC, poly(PA-*co*-ANI)/TiC, PANI/TiC nanocomposites and the pure PANI, pure PPA and TiC, the thermal analyses of samples were tested, the results are shown in Fig. 4. In the first stage, the weight loss starting practically from room temperature to 110 °C is due to the loss of water molecules and moisture present in the samples. Note that the degradation of nanocomposites is slower than that of pure polymers with the temperature increase, and the thermal stability of PPA/TiC is higher than that of poly(PA-*co*-ANI)/TiC and that PANI/TiC respectively; these results also demonstrates that the

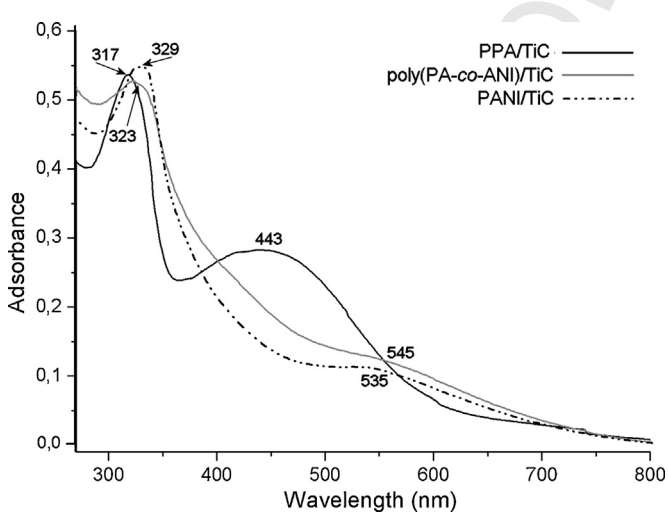

Fig. 3. UV–vis spectra of PPA/TiC, poly(PA-*co*-ANI)/TiC and PANI/TiC nanocomposites.

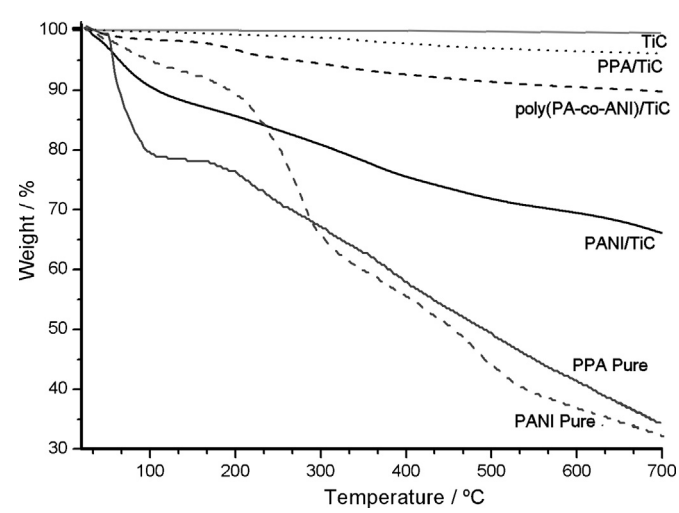

Fig. 4. Thermogravimetric analysis (TGA) of nanocomposites (PPA/TiC, poly(PA-*co*-ANI)/TiC and PANI/TiC), pure polymers (PPA and PANI) and TiC nanoparticles obtained in nitrogen atmosphere at heating rate of 10 °C/min.

Please cite this article in press as: I. Radja, et al., Characterization and electrochemical properties of conducting nanocomposites synthesized from *p*-anisidine and aniline with titanium carbide by chemical oxidative method, Synthetic Met. (2015), http://dx.doi.org/10.1016/j.synthmet.2015.01.028

Table 3
The amount of nanocomposites at 20 °C, 700 °C and the percentage of the amount formed on TiC nanoparticule.

Samples	w_i (g) at 20 °C	w_f (g) at 700 °C	Δw %
PPA/TiC	7.06	6.71	5.0
Poly(PA-*co*-ANI)/TiC	6.92	6.06	12.4
PANI/TiC	4.16	2.29	44.9

thermo stability of nanocomposites depends on the polymer type used (structure of the polymers and the interaction between two components) [41].

The thermal behaviour of PPA pure is similar to that of PANI pure and exhibits a four-stage decomposition pattern. In the first stage, is due to the loss of water molecules and moisture present in the polymer. The second- and third-stage losses that occur from 110 °C to 350 °C are attributed to the loss of the dopant from the polymer chains. While the fourth stage loss from 350 °C to 600 °C is the result of the complete degradation and decomposition of the polymer backbone [42].

The results implied that the incorporation of nanoparticules TiC into polymer resulted in the improvement of the thermal stability of nanocomposites.

One of the common uses of TGA analysis in the technology is to determine the polymer amount of a nanocomposite. The definition of each sample is based on its relative volatility. The success of the method depends on each component having a different thermal stability range in an inert atmosphere. The amount of polymer was calculated by difference between the initial amount to 20 °C and after a temperature 700 °C (the degradation behavior), according to

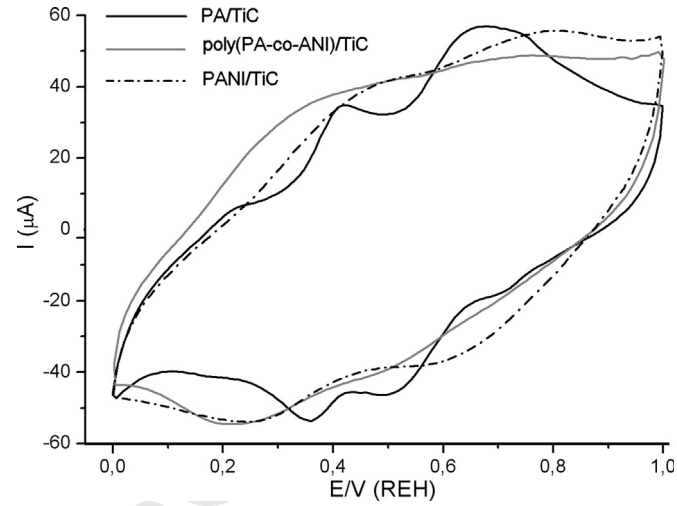

Fig. 5. Cyclic voltammograms recorded for a graphite carbon electrode covered by PPA/TiC, poly(PA-*co*-ANI)/TiC and PANI/TiC nanocomposites in 1 M $HClO_4$ solution. Scan rate 50 mV/s.

the following equation:

$$\Delta w = \frac{w_i - w_f}{w_i} \times 100 \quad (2)$$

where w_i and w_f are the amounts of polymer at 20 °C and at 700 °C (g), respectively. Δw is the percentage of the amount of polymer formed on TiC (see data in Table 3).

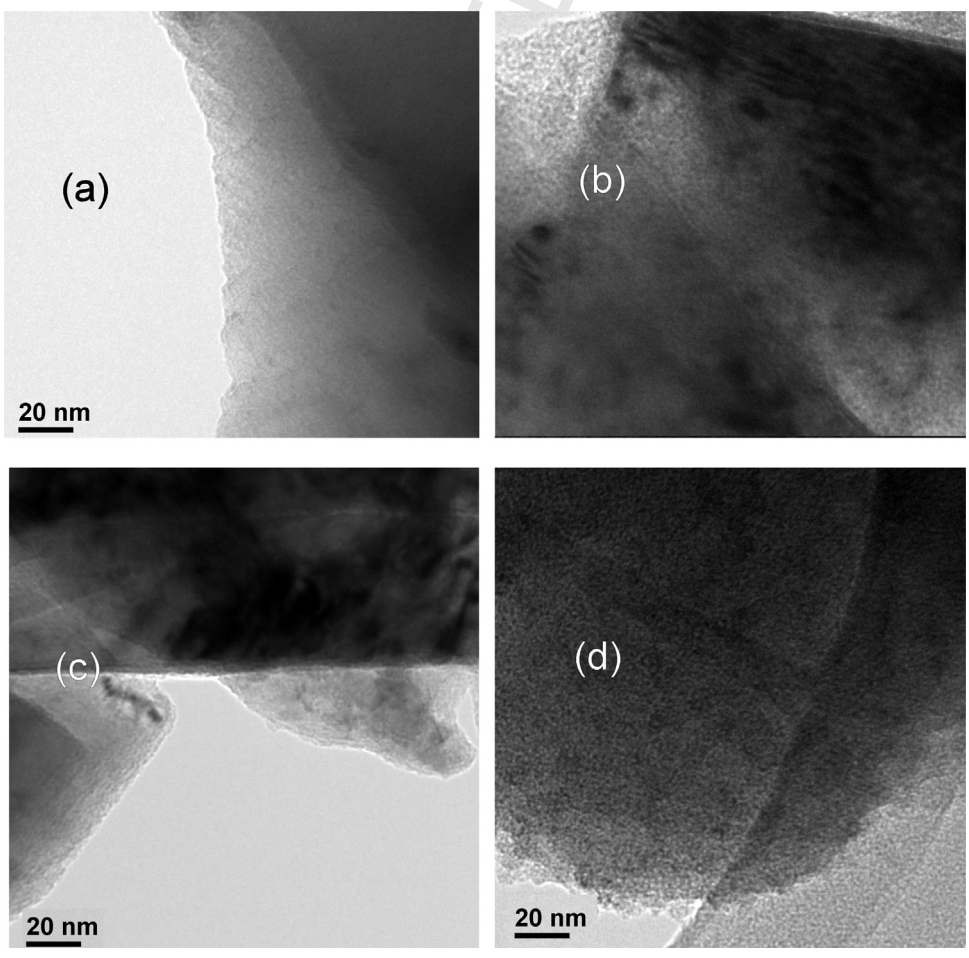

Fig. 6. TEM images of: (a) TiC nanoparticle, (b) PPA/TiC, (c) poly(PA-*co*-ANI)/TiC and (d) PANI/TiC nanocomposites.

Please cite this article in press as: I. Radja, et al., Characterization and electrochemical properties of conducting nanocomposites synthesized from *p*-anisidine and aniline with titanium carbide by chemical oxidative method, Synthetic Met. (2015), http://dx.doi.org/10.1016/j.synthmet.2015.01.028

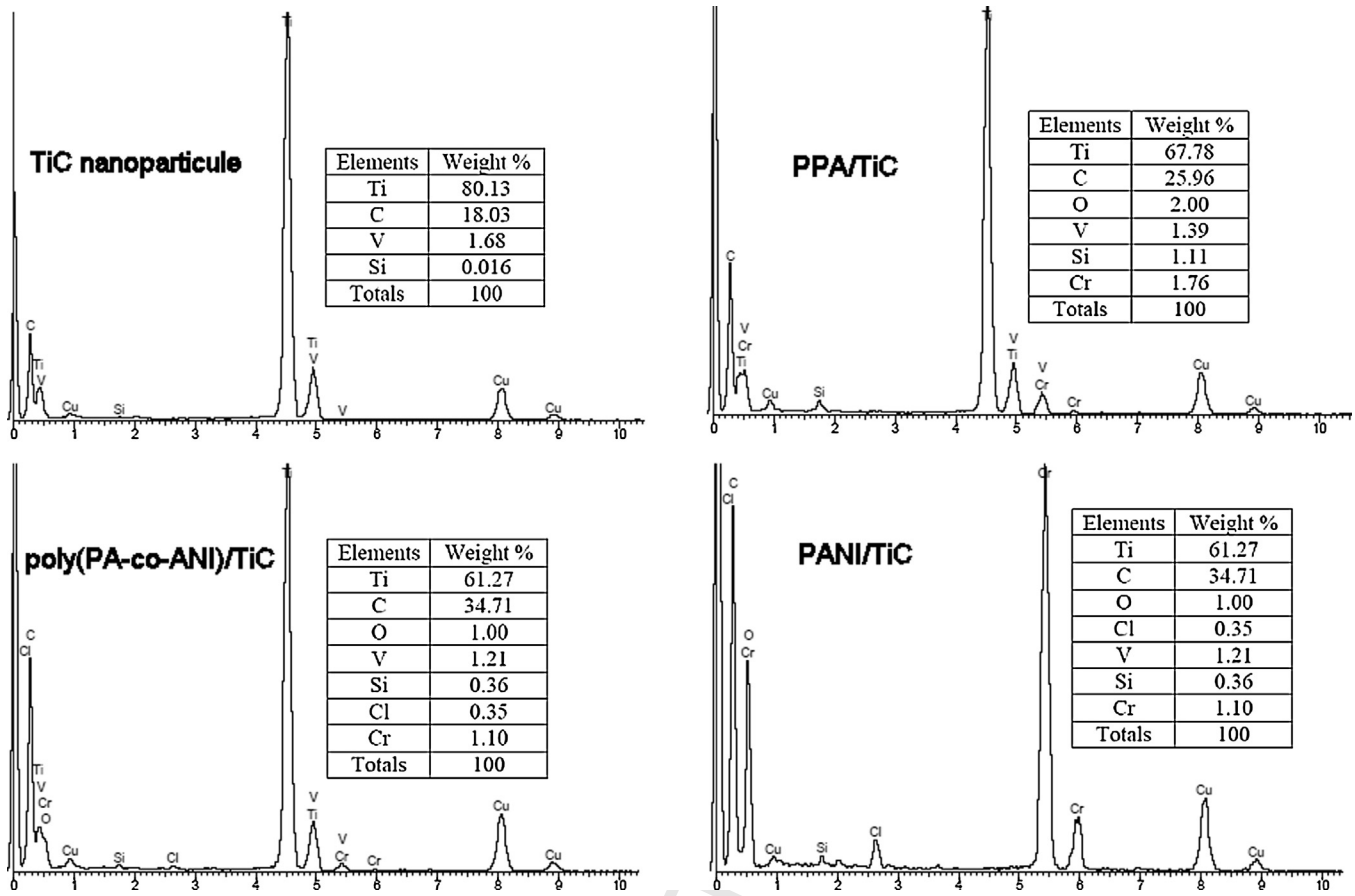

Fig. 7. EDS spectra of TiC nanoparticule, PPA/TiC, poly(PA-*co*-ANI)/TiC and PANI/TiC nanocomposites.

3.6. Electrochemical properties

Cyclic voltammetry experiments were performed to test the electroactivity of the polymers. Fig. 5 shows the steady voltammograms for polymers from PPA/TiC, poly(PA-*co*-ANI)/TiC and PANI/TiC samples, obtained in 1 M $HClO_4$ solution at a scan rate of 50 mV s^{-1}. In the case of PANI/TiC nanocomposite, two overlapped redox processes are observed. The first one appears at 0.45/0.27 V, which results in a potential peak separation (ΔE_p) close to 180 mV; the second process is observed at 0.77/0.59 V and gives an ΔE_p value of 180 mV. The first redox process is due to the oxidation of the leucoemeradilneto emeraldine form and the second one to the oxidation of the emeraldine to pernigraniline of polyaniline [43,44]. The voltammetric profile of copolymer poly(PA-*co*-ANI)/TiC also show two redox process, however in this case the two processes are more overlapped.

The voltammetric profile for PPA/TiC nanocomposite shows three redox process, the first centered at 0.22/0.36 V gives a ΔE_p value of 140 mV; the second processes at 0.41/0.50 V (ΔE_p = 90 mV) and finally, the third process centered at 0.66/0.70 V with a ΔE_p value of 40 mV.

3.7. Transmission electron microscopy (TEM)

Fig. 6 shows the TEM images of the nanocomposites (PPA/TiC, poly(PA-*co*-ANI)/TiC and PANI/TiC) and nanoparticle (pure TiC), and after evaporation of the solvent. In Fig. 6(b–d), one can observe the formation of a homogeneous film of polymer particles, whereas in Fig. 6(a), we present a TEM image of pure TiC nanoparticles. However, as it can be seen in Fig. 6(d), a more fibrous structure seems to be associated to the PANI/TiC nanocomposite [45].

Energy dispersive spectroscopy (EDS) analysis of nanocomposites and nanoparticule revealed the presence of Ti and C elements peaks which confirmed the existence of TiC nanoparticles (Fig. 7). In this paper, the spectra of PPA/TiC, poly(PA-*co*-ANI)/TiC and PANI/TiC nanocomposites indicates that the intensity of Ti decreased; on the contrary, the intensity of C increased, which demonstrates that the TiC nanoparticles are successfully coated by the polymers [46]. However, the elements weight contains signals of Ti, C, Cl and O together with those of the nanocomposites (Tables in Fig. 7).

3.8. Mechanism of formation of polymer/TiC nanocomposites

Scheme 1 shows the proposed reaction scheme for the deposition of polymer on the surface of TiC nanoparticles and the chemical oxidative polymerisation of monomers (PA and/or ANI) with APS to form partially encapsulated nanocomposite particles (PA/TiC, poly(PA-*co*-ANI)/TiC and PANI/TiC).

There are a bond interaction at the interface between TiC nanoparticles and polymer. Hydrogen bonds can be formed via the amido $-NH_2$ group in the monomers (PA and/or ANI) and the large amount of hydroxides produced on the surface of TiC nanoparticles when they come into contact with water.

Simultaneously, the N atom in the $-NH_2$ group has a lone pair of electrons and can be coordinated with the Ti atom. Thus there may be hydrogen bonding and coordinate bonding between TiC and polymer.

When the TiC nanoparticles are introduced into the reaction mixture, the surfaces of individual nanoparticles act as template

Please cite this article in press as: I. Radja, et al., Characterization and electrochemical properties of conducting nanocomposites synthesized from *p*-anisidine and aniline with titanium carbide by chemical oxidative method, Synthetic Met. (2015), http://dx.doi.org/10.1016/j.synthmet.2015.01.028

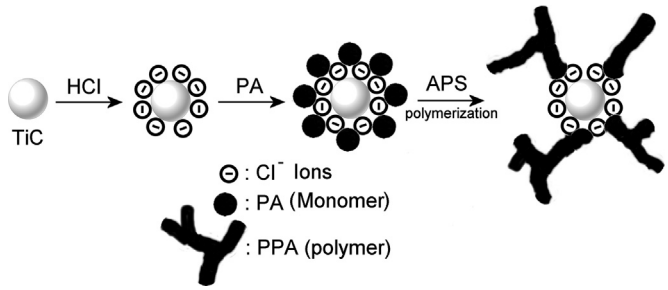

Scheme 1. Scheme of polymer/TiC nanocomposites preparation.

areas for the growth of polymer. Due to the polymerization in the acidic medium, the surface of the TiC is positively charged and therefore, adsorption of anions such as Cl^- may compensate the positive charges on the TiC surface.

It is assumed that oligomers (PA and/or ANI) produced at the beginning of the reaction because of their reduced solubility in water, are deposited on the TiC surfaces. As a consequence, the interactions between adsorbed anions and oligomers initiate the growth of polymer chains on the TiC surface. It is known that the polymerization of aniline and its substituted derivatives is auto-accelerated process [47]. That is, the polymer formation is preferred in the region where some polymer has already been produced. This leads to a formation of the polymer layer on the surface of the TiC (as shown in Scheme 1).

4. Conclusions

Polymer/TiC nanocomposites were prepared from in situ intercalative oxidative polymerization of *p*-anisidine and/or aniline with TiC nanoparticles. The synthesized nanocomposites were characterized by X-ray diffraction pattern (XRD), fourier transform infrared (FTIR), transmission electron microscopy (TEM), energy dispersive spectroscopy (EDS), thermogravimetric analysis (TGA) and electrical conductivity techniques. The electrochemical behavior of polymer/TiC shows that these nanocomposites exhibits a redox processes indicate that the polymerisation on TiC nanoparticles produces electroactive polymers.

Acknowledgements

This work was supported by the National Assessment and Planning Committee of the University Research (CNEPRU), and the Directorate General of Scientific Research and Technological Development (DGRSDT) of Algeria. Financial support from the Generalitat Valenciana (PROMETEO2013/038) is acknowledged.

References

[1] R.A. Irgashev, A.A. Karmatsky, S.A. Kozyukhin, V.K. Ivanov, A. Sadovnikov, V.V. Kozik, V.A. Grinberg, V.V. Emets, G.L. Rusinov, V.N. Charushin, A facile and convenient synthesis and photovoltaic characterization of novel thieno[2,3-b] indole dyes for dye-sensitized solar cells, Synth. Met. 199 (2015) 152–158.
[2] Y. Li, K. Fan, H. Ban, M. Yang, Bilayer-structured composite sensor based on polyaniline and polyelectrolyte for sensitive detection of low humidity, Synth. Met. 199 (2015) 51–57.
[3] S. Gunes, H. Neugebauer, N.S. Sariciftci, Conjugated polymer-based organic solar cells, Chem. Rev. 107 (2007) 1324–1338.
[4] H. Hoppe, N.S. Sariciftci, Organic solar cells: an overview, J. Mater. Res. 19 (2004) 1924–1945.
[5] Y.N. Qi, F. Xu, L.X. Sun, J.L. Zeng, Y.Y. Lui, Thermal stability and glass transition behavior of PANI/α-Al_2O_3 composites, J. Therm. Anal. Calorim. 94 (2008) 553–557.
[6] Y. Furukawa, F. Ueda, Y. Hyodo, I. Harada, T. Nakajima, T. Kawagoe, Vibrational spectra and structure of polyaniline, Macromolecules 21 (1998) 1297–1305.
[7] E. Mitchell, J. Candler, F. De Souza, R.K. Gupta, B.K. Gupta, L.F. Dong, High performance supercapacitor based on multilayer of polyaniline and graphene oxide, Synth. Met. 196 (2015) 214–218.
[8] S. Uppugalla, U. Male, P. Srinivasan, Design and synthesis of heteroatoms doped carbon/polyaniline hybrid material for high performance electrode insupercapacitor application, Electrochim. Acta 146 (2014) 242–248.
[9] W. Chen, Q. Xu, Y.S. Hu, L.Q. Mai, Q.Y. Zhu, Effect of modification by poly (ethylene oxide) on the reversibility of insertion/extraction of Li^+ ion in V_2O_5 xerogel films, J. Mater. Chem. 12 (2002) 1926–1929.
[10] X.F. Yang, G.C. Wang, R.Y. Wang, X.W. Li, A novel layered manganese oxide/poly (aniline-*co*-*o*-anisidine) nanocomposite and its application for electrochemical supercapacitor, Electrochim. Acta 55 (2010) 5414–5419.
[11] P. Judeinstein, C. Sanchez, Hybrid organic–inorganic materials: a land of multidisciplinarity, J. Mater. Chem. 6 (1996) 511–525.
[12] G. Mercouri, M.G. Kanatzidis, C. Wu, Conductive-polymer bronzes. Intercalated polyaniline in vanadium oxide xerogels, J. Am. Chem. Soc. 111 (1989) 4139–4141.
[13] A. Zehhaf, E. Morallon, A. Benyoucef, Polyaniline/montmorillonite nanocomposites obtained by in situ intercalation and oxidative polymerization in cationic modified-clay (sodium copper and iron), J. Inorg. Organomet. Polym. 23 (2013) 1485–1491.
[14] I. Toumi, A. Benyoucef, A. Yahiaoui, C. Quijada, E. Morallon, Effect of the intercalated cation-exchanged on the properties of nanocomposites prepared by 2-aminobenzene sulfonic acid with aniline and montmorillonite, J. Alloys Compd. 551 (2013) 212–218.
[15] Z. Zhang, M. Wan, Nanostructures of polyaniline composites containing nano-magnet, Synth. Met. 132 (2003) 205–212.
[16] Y. He, A novel emulsion route to sub-micrometer polyaniline/nano-ZnO composite fibers, Appl. Surface Sci. 249 (2005) 1–6.
[17] S. Wang, Z. Tan, Y. Li, L. Sun, T. Zhang, Synthesis, characterization and thermal analysis of polyaniline/ZrO_2 composites, Therm. Chim. Acta 441 (2006) 191–194.
[18] M.O. Ansari, F. Mohammad, Thermal stability of HCl-doped-polyaniline and TiO_2 nanoparticles-based nanocomposites, J. Appl. Polym. Sci. 124 (2012) 4433–4442.
[19] Y. Shoji, F. Ohashi, Y. Ohnishi, T. Nonami, Synthesis of polyaniline–montmorillonite nanocomposites by the mechanochemical intercalation method, Synth. Met. 145 (2004) 265.
[20] S. Mohapatra, D.K. Mishra, S.K. Singh, Microscopic and spectroscopic analyses of TiC powder synthesized by thermal plasma technique, Powder Technol. 237 (2013) 41–45.
[21] H. Lin, B. Tao, J. Xiong, Q. Li, Using a cobalt activator to synthesize titanium carbide (TiC) nanopowders, Int. J. Refract. Metals Hard Mater. 41 (2013) 363–365.
[22] Y. Liu, K. Oshima, T. Yamauchi, M. Shimomura, S. Miyauchi, Temperature-conductivity characteristics of the composites consisting of fractionated poly (3-hexylthiophene) and conducting particles, J. Appl. Polym. Sci. 77 (2000) 3069–3076.
[23] Y.K. Sung, F. El-Tantawy, Novel smart polymeric composites for thermistors and electromagnetic wave shielding effectiveness from TiC loaded styrene-butadiene rubber, Macromol. Res. 10 (2002) 345–358.
[24] F. El-Tantawy, New double negative and positive temperature coefficients of conductive epdm rubber TiC ceramic composites, Eur. Polym. J. 38 (2002) 567–577.
[25] C.G. Raptis, A. Patsidis, G.C. Psarras, Electrical response and functionality of polymer matrix-titanium carbide composites, eXPRESS Polym. Lett. 4 (2010) 234–243.
[26] F. El-Tantawy, Joule heating treatments of conductive butyl rubber/ceramic superconductor composites: a new way for improving the stability and reproducibility, Eur. Polym. J. 37 (2001) 565–574.
[27] C. Bian, G. Xue, Nanocomposites based on rutile-TiO_2 and polyaniline, Mater. Lett. 61 (2007) 1299–1302.
[28] M.K. Rasha, Synthesis characterization, magnetic and electrical properties of the novel conductive and magnetic polyaniline/$MgFe_2O_4$ nanocomposite having the core–shell structure, J. Alloys Compd. 509 (2011) 9849–9857.
[29] A. Belmokhtar, A. Benyoucef, A. Yahiaoui, C. Quijada, E. Morallon, Studies on the conducting nanocomposite prepared by polymerization of 2-aminobenzoic acid with aniline from aqueous solutions in montmorillonite, Synth. Met. 162 (2012) 1864–1870.
[30] J. He, N.W. Duffy, J.M. Pringle, Y.B. Cheng, Conducting polymer and titanium carbide-based nanocomposites as efficient counter electrodes for dye-sensitized solar cells, Electrochim. Acta 105 (2013) 275–281.
[31] H.P. Klug, L.E. Alexander, X-Ray Diffraction Procedures for Polycrystalline and Amorphous Materials, Wiley, New York, 1954.
[32] R.A. Salih, Synthesis, identification and study of electrical conductivity of the doped poly(*p*-anisidine), J. Mater. Environ. Sci. 3 (2012) 50–56.
[33] S.G. Pawar, S.L. Patil, M.A. Chougule, A.T. Mane, D.M. Jundale, V.B. Patil, Synthesis and characterization of polyaniline:TiO_2 nanocomposites, Int. J. Polym. Mater. 59 (2010) 777–785.
[34] D. Patil, P. Patil, Y.K. Seo, Y.K. Hwang, Poly(*o*-anisidine)–tin oxide nanocomposite: synthesis, characterization and application to humidity sensing, Sens. Actuators B: Chem. 148 (2010) 41–48.
[35] D.R. Yei, S.W. Kuo, H.K. Fu, F.C. Chang, Enhanced thermal properties of PS nanocomposites formed from montmorillonite treated with surfactant/cyclodextrin inclusion complex, Polymer 46 (2005) 741–750.
[36] W.M.A.T. Bandara, D.M.M. Krishantha, J.S.H.Q. Perera, R.M.G. Rajapakse, D.T.B. Tennakoon, Preparation, characterization and conducting properties of nanocomposites of successively intercalated polyaniline in montmorillonite, J. Compos. Mater. 39 (2005) 759–775.

[37] D. Lee, K. Char, S.W. Lee, Y.W. Park, Structural changes of polyaniline/montmorillonite nanocomposites and their effects on physical properties, J. Mater. Chem. 13 (2003) 2942–2947.
[38] K. Samrana, A. Shahzada, P. Jiri, P. Josef, M.J. Yogesh, Polyaniline-sodium montmorillonite clay nanocomposites: effect of clay concentration on thermal structural, and electrical properties, J. Mat. Sci. 47 (2012) 420–428.
[39] T. Abdiryim, R. Jamal, I. Nurulla, Doping effect of organic sulphonic acids on the solid-state synthesized polyaniline, J. Appl. Polym. Sci. 105 (2007) 576–584.
[40] P. Mokreva, D. Tsocheva, G. Ivanova, L. Terlemezyan, Copolymers of aniline and o-methoxyaniline: synthesis and characterization, J. Appl. Polym. Sci. 98 (2005) 1822–1828.
[41] S. Bitao, M. Shixiong, S. Shixiong, T. Yongchun, B. Jieet, Synthesis and characterization of conductive polyaniline/TiO_2 composite nanofibers, Front. Chem. China 2 (2007) 123–126.
[42] M.C. Gupta, S.S. Umare, Studies on poly(o-methoxy anilines), Macromolecules 25 (1992) 138–142.
[43] F. Chouli, A. Zehhaf, A. Benyoucef, Synthesis and characterization of conducting composites obtained from 2-methylaniline and aniline with activated carbon, Macromol. Res. 22 (2014) 26–31.
[44] M. Khaldi, A. Benyoucef, S. Bousalem, A. Yahiaoui, E. Morallon, Synthesis, characterization and conducting properties of nanocomposites of successively intercalated 2-aminophenol with aniline in modified-montmorillonite, J. Inorg. Organomet. Polym. Mater. 24 (2014) 267–274.
[45] K.G.B. Alves, J.F. Felix, E.F. de Melo, C.G. dos Santos, C.A.S. Andrade, C.P. de Melo, Characterization of ZnO/polyaniline nanocomposites prepared by using surfactant solutions as polymerization media, J. Appl. Polym. Sci. 125 (2012) 141–147.
[46] H.Y. Zhang, Y.Q. Hu, Preparation of carbon coated Fe_3O_4 nanoparticles and their application for solid-phase extraction of polycyclic aromatic hydrocarbons from environmental water samples, J. Chromatogr. A 1217 (2010) 4757–4764.
[47] K. Tzou, R.V. Gregory, Kinetic study of the chemical polymerization of aniline in aqueous solutions, Synth. Met. 47 (1992) 267–277.

Please cite this article in press as: I. Radja, et al., Characterization and electrochemical properties of conducting nanocomposites synthesized from *p*-anisidine and aniline with titanium carbide by chemical oxidative method, Synthetic Met. (2015), http://dx.doi.org/10.1016/j.synthmet.2015.01.028